Hole superconductivity in oxides: A two-band model

J. E. Hirsch and F. Marsiglio*
Department of Physics, University of California at San Diego, La Jolla, California 92093
(Received 29 June 1990; revised manuscript received 9 July 1990)

The role of the Cu $d_{x^2-y^2}$ orbitals in the theory of hole superconductivity in oxides is considered. We use a two-band model of the type introduced by Suhl *et al.*, describing a purely oxygen band coupled to a copper-oxygen band. The pure O band is nearly full, and the Cu-O band is nearly half-filled in the parameter range of interest. It is found that many of the features of the single-band hole-pairing description of the oxides survive the generalization to the two-band model. The new feature of the present model is the existence of a second, smaller, superconducting gap associated with the Cu-O band. This can give rise to features in the tunneling characteristics that reproduce certain experimental observations. The effect of the second gap in the specific-heat behavior below T_c is also examined, and deviations from exponential behavior at intermediate temperatures are found. It is also proposed that this model provides an explanation for the anomalous behavior found in the Hall coefficient just below T_c.

I. INTRODUCTION

Superconductivity in oxides has recently been described as originating in pairing of oxygen hole carriers in a single band arising from direct overlap of oxygen orbitals, presumably of $p\pi$ character.[1] The mechanism that pairs oxygen holes, an enhanced hopping amplitude for a hole when another hole is nearby, arises when direct hopping of holes between O^{2-} anions occurs.[2] The purpose of this paper is to incorporate into this description the relevant degrees of freedom associated with Cu $d_{x^2-y^2}$ and O p_σ orbitals. It is likely that a band arising from these orbitals crosses the Fermi level in the relevant doping range, so that inclusion of these charge carriers is necessary for a complete description.

In the following we call the band arising from direct overlap of oxygen $p\pi$ orbitals the O band (or band 1) and the band arising from Cu $d_{x^2-y^2}$– O p_σ orbitals the Cu band (or band 2). A schematic picture of these orbitals is given, for example, in Ref. 3. In the undoped case (La_2CuO_4 or $YBa_2Cu_3O_{6.5}$) the system is an antiferromagnetic insulator, corresponding to the O band being full and the Cu band being half-full, with a Mott-Hubbard gap arising from Coulomb interactions. We shall not attempt here a description of how the gap closes as the system is doped. Experiments show that antiferromagnetism disappears rapidly with doping,[4] and we will assume that the system becomes a Fermi liquid, with conduction occurring through both bands, the effective bandwidths being presumably renormalized by interaction effects. Figure 1 shows schematically the position of the Fermi level in the undoped and slightly doped systems.

We adopt a semiphenomenological description. It is our point of view that superconductivity in these systems is driven by the strong attractive interaction in the O band. The simplest way to describe this situation is to couple the two bands by a reduced interaction of the form

$$H_{\text{Cu-O}} = \sum_{kk'} V^{12}_{kk'} (c^\dagger_{k\uparrow} c^\dagger_{-k\downarrow} d_{-k'\downarrow} d_{k'\uparrow} + d^\dagger_{k\uparrow} d^\dagger_{-k\downarrow} c_{-k'\downarrow} c_{k'\uparrow}) , \quad (1)$$

where c and d operators correspond to O and Cu bands, respectively. Such an interaction was introduced by Suhl *et al.*[5] to describe superconductivity in a two-band system. If the interactions in the O band cause the development of an anomalous expectation value $\langle c^\dagger_{k\uparrow} c^\dagger_{-k\downarrow} \rangle$,

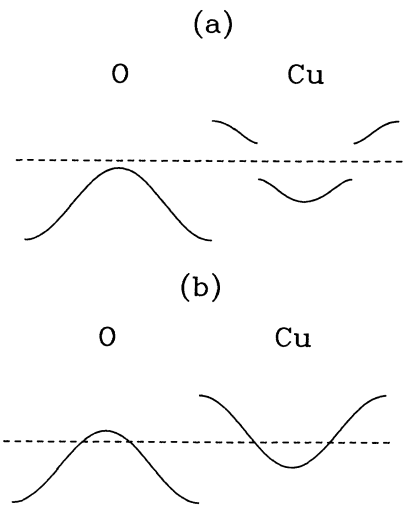

FIG. 1. (a) In the undoped system the oxygen band is completely filled with electrons and the Cu band is half-filled with a presumed Mott-Hubbard gap. (b) Upon removal of electrons the Fermi level shifts to below the top of the O band, while in the Cu band the gap disappears and the band is less than half-filled. The hole picture adopted in this paper is obtained by turning the figure upside down. Doping with holes would then correspond to raising the Fermi level.

such a term in Eq. (1) will "drive" the development of a corresponding expectation value $\langle d_{-k\downarrow} d_{k\uparrow} \rangle$ in the Cu band. One may intuitively expect that the coupling of the two subsystems will not strongly affect the critical temperature, and that the order parameter in the second subsystem could be much smaller than in the first. As we will see, such is the situation in our model.

Microscopically, an interaction of the form Eq. (1) could arise from an intra-atomic exchange matrix element

$$J = \int d^3r \; d^3r' \phi^*_{p_x}(r) \phi^*_{p_y}(r') \frac{e^2}{|r-r'|} \phi_{p_x}(r') \phi_{p_y}(r) \tag{2}$$

between p_x and p_y orbitals on an oxygen ion. The d operators in Eq. (1) are a linear combination of Cu $d_{x^2-y^2}$ and O p_σ orbitals, and thus we may expect the interaction equation (2) to give rise to a term of the form Eq. (1). Many other interaction terms surely occur, which we assume renormalize our basic parameters but do not qualitatively change the physics.

The model considered here has many features in common with the single-band model of Ref. 1, that appear to reproduce various experimental observations in the oxides: doping dependence of T_c, pressure dependence of T_c, gap isotropy, etc. New features of the present model are related to the presence of a second gap associated with the Cu band, which is smaller than the gap in the O band. This can give rise to structure in the tunneling characteristics at low temperatures that resemble recent experimental observations.[6,7] In addition, the existence of the second gap causes the gap in the tunneling characteristic to "fill in" as the temperature is raised, faster than in a single-band model, which may explain some observations.[4] The specific heat at low temperatures displays nonexponential behavior due to the presence of the second gap, in qualitative agreement with some observations.[4] Finally, it is proposed that this model contains the explanation for the anomalous behavior of the Hall coefficient just below T_c observed:[8,9] the Hall coefficient is negative for small fields and becomes positive for larger fields. We will show how this behavior arises in the present model within a simple treatment.

II. FORMALISM

We consider a reduced Hamiltonian of the form

$$H = \sum_{k\sigma} (\varepsilon^1_{k\sigma} - \mu) c^\dagger_{k\sigma} c_{k\sigma} + \sum_{k\sigma} (\varepsilon^2_{k\sigma} - \varepsilon_0 - \mu) d^\dagger_{k\sigma} d_{k\sigma} + \sum_{kk'} V^{11}_{kk'} c^\dagger_{k\uparrow} c^\dagger_{-k\downarrow} c_{-k'\downarrow} c_{k'\uparrow}$$
$$+ \sum_{kk'} V^{22}_{kk'} d^\dagger_{k\uparrow} d^\dagger_{-k\downarrow} d_{-k'\downarrow} d_{k'\uparrow} + \sum_{kk'} V^{12}_{kk'} (c^\dagger_{k\uparrow} c^\dagger_{-k\downarrow} d_{-k'\downarrow} d_{k'\uparrow} + d^\dagger_{k\uparrow} d^\dagger_{-k\downarrow} c_{-k'\downarrow} c_{k'\uparrow}) , \tag{3}$$

and assume for simplicity a flat density of states in both bands, of bandwidth D_i. The energies $\varepsilon^i_{k\sigma}$ are measured from the center of each band, and ε_0 is the shift in the Cu band relative to the O band. We adopt the convention that the operators describe holes in the bands, to be consistent with our previous treatment of the single-band model. Taking $\varepsilon_0 = D_1/2$ the center of the Cu band coincides with the bottom of the O band, i.e., for $\mu = -D_1/2$ at $T=0$ the O band is just empty of holes and the Cu band is half-full.

We will not be interested in a detailed description of the interactions in the Cu band, as we believe they are not essential to the superconductivity; in fact, in much of this paper we will examine the situation $V^{22}_{kk'} \equiv 0$, i.e., assume the interactions in the Cu band are negligible except for renormalizing the other interactions in the problem. Nevertheless, for generality here we take the interactions in both bands to be of the form used in Ref. 1 for the single-band model:

$$V^{ii}_{kk'} = U_i + K_i \left[\frac{\varepsilon^i_k}{D_i/2} + \frac{\varepsilon^i_{k'}}{D_i/2} \right] + W_i \frac{\varepsilon^i_k}{D_i/2} \frac{\varepsilon^i_{k'}}{D_i/2} , \tag{4}$$

with the parameters U_i, W_i, and K_i arising from on-site repulsion, nearest-neighbor repulsion and modulated hopping, respectively. As the simplest possible coupling between both bands we use a structureless form

$$V^{12}_{kk'} = V_{12} . \tag{5}$$

The mean-field solution of this problem is a straightforward generalization of the case discussed by Suhl *et al.*[5] Two gaps are obtained, both of the form

$$\Delta_i(\varepsilon) = \Delta^m_i \left[c_i - \frac{\varepsilon}{D_i/2} \right] \tag{6}$$

as in the single-band case.[1] The parameters c_i and Δ^m_i are determined by the four self-consistency conditions

$$1 = K_i [I_1(i) + c_i I_0(i)] - W_i [I_2(i) + c_i I_1(i)] , \tag{7a}$$

$$\Delta^m_i c_i = \Delta^m_i K_i [I_2(i) + c_i I_1(i)] - \Delta^m_i U_i [I_1(i) + c_i I_0(i)] + \Delta^m_j V_{ij} [I_1(j) + c_j I_0(j)] , \tag{7b}$$

for $i = 1,2$, with $j \neq i$ in Eq. (7b). The integrals $I_l(i)$ are given by

$$I_l(i)=\int d\varepsilon g_i(\varepsilon)\left[\frac{-\varepsilon}{D_i/2}\right]^l\frac{1-2f(E_i)}{2E_i} \tag{8}$$

as in the single band case, with f the Fermi function,

$$E_i=\sqrt{(\varepsilon-\varepsilon_0^i-\mu)^2+\Delta_i(\varepsilon)^2} \tag{9}$$

and $\varepsilon_0^1=0$, $\varepsilon_0^2=\varepsilon_0$. We will use for the densities of states

$$g_i(\varepsilon)=\begin{cases}\dfrac{1}{D_i} & -\dfrac{D_i}{2}\le\varepsilon\le\dfrac{D_i}{2}\\ 0 \text{ otherwise .}\end{cases} \tag{10}$$

The critical temperature is determined by the single equation

$$\prod_{i=1}^{2}\{1+U_iI_0(i)-2K_iI_1(i)+W_iI_2(i)-(K_i^2-W_iU_i)[I_0(i)I_2(i)-I_1(i)^2]=V_{12}^2\prod_{i=1}^{2}\{I_0(i)+W_i[I_0(i)I_2(i)-I_1(i)^2]\} . \tag{11}$$

Both Eqs. (7) and (11) reduce to the single-band equations when $V_{12}\to 0$. Finally, the number of particles in each band is given by

$$n_i=1-\int d\varepsilon g_i(\varepsilon)\frac{\varepsilon-\varepsilon_0^i-\mu}{E_i}[1-2f(E_i)] . \tag{12}$$

Thus, within our simplified model the two bands are only coupled through the self-consistency condition equation (7). Once it is solved for the parameters Δ_i^m, c_i, observables are simply obtained by summing over the corresponding quantities for both bands. At a single critical temperature determined by Eq. (11) both gaps go simultaneously to zero, as in the model of Suhl *et al.*

In the following section we discuss the behavior of this model for some simple examples to illustrate the effect of the second band on the results obtained for the single-band model. In Sec. IV we discuss the behavior of the Hall coefficient in this model and we conclude in Sec. V with a discussion.

III. RESULTS

For definiteness we will present results for only a few parameter sets. Many of the trends as a function of doping, for example, are similar to those already studied in the single-band case. Throughout this section we keep the bandwidths of the two bands equal, $D_1=D_2=0.5$ eV, and for simplicity set $W_1=W_2=0$. As shown in Ref. 1, a nearest-neighbor repulsion W does not qualitatively alter the results. In the next subsection we present results for various quantities for a simplified case (noninteracting Cu band), and in the following subsection we discuss how the results depend on parameter values.

A. A simple example

As a simple example to illustrate the properties of the two-band model we assume no interactions in the electron band, i.e., $U_2=K_2=0$. We choose $U_1=5$ eV in the O band and $K_1=1.59$ eV to give a maximum T_c in the desirable range, $T_c\sim 94$ K. (This corresponds to a hopping interaction $\Delta t=K_1/8=0.20$ eV.) The interaction coupling the two bands is taken as $V_{12}=0.2$ eV. In Fig. 2 we plot T_c as a function of the hole concentration in the oxygen band (n_1). Also shown is the single-band result obtained with the same parameters except that $V_{12}=0$. The shape of the T_c vs n_1 curve is similar in the two cases. An overall enhancement of T_c occurs in the two-band model. We wish to emphasize, however, that this increase in T_c will presumably be offset by other interband Coulomb interactions not included in our model. The dominant source of T_c remains the same as in the single-band model: the modulated hopping term in the oxygen band with coefficient K_1. As we shall see, this behavior persists even when strongly repulsive interactions are present in the copper band.

In Fig. 2 we have omitted the part of the T_c vs n_1 curve near $n_1=0$. At $T=0$ as $n_1\to 0$, the occupancy of the copper band, n_2, approaches unity. However, at finite temperature, thermal smearing in principle allows an occupancy in the copper band of less than one, which

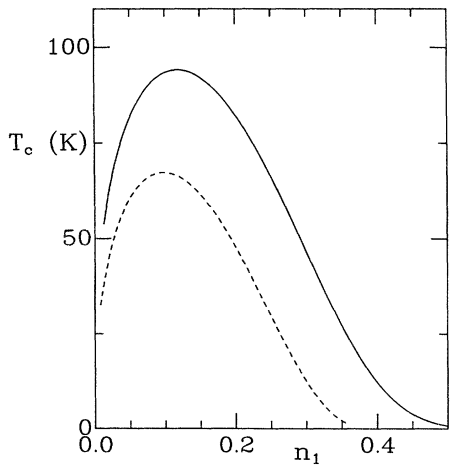

FIG. 2. T_c vs n_1 (hole concentration in the oxygen band) for the two-band model (solid line) and the single-band model (dashed line). We have used $D_1=D_2=0.5$ eV, $K_1=1.59$ eV, $U_1=5$ eV, and $U_2=K_2=0$. In the two-band model, $V_{12}=0.2$ eV.

is physically incorrect, so we have restricted the curve in Fig. 2 using the condition $n_2 \geq 1$. As $n_2 \to 1$ ($n_1 \to 0$) the Mott-Hubbard gap will develop and give rise to an insulating state; this development is beyond the scope of this paper. For reference we show in Fig. 3 n_1 and n_2 vs chemical potential at $T=0$.

Below the superconducting transition temperature gaps develop in the Cu and O bands [Eq. (6)]. The gap function in the O band displays strong energy dependence as found in the single-band model.[1] As an example, at the density where T_c peaks in Fig. 2, $n_1=0.12$, we find $\Delta_1^m=36.9$ meV, $c_1=-0.445$. In contrast, the Cu gap has no energy dependence due to the fact that we have taken $K_2=0$ [i.e., in Eq. (6) $\Delta_2^m \to 0$, $c_2 \to \infty$ with $\Delta_2^m c_2$ finite $=4.67$ meV in this case]. The quasiparticle gaps are obtained by minimizing the energy dispersion relation Eq. (9) as in the single-band case:

$$\Delta_{0i} = \frac{\Delta_i(\mu+\varepsilon_0^i)}{\left[1+\left[\frac{\Delta_i^m}{D_i/2}\right]^2\right]^{1/2}} . \tag{13}$$

In Fig. 4 we show results for the temperature dependence of these two gaps. Both gaps appear BCS-like, in that they display $\sim\sqrt{1-T/T_c}$ dependences near T_c and become exponentially flat as $T \to 0$. The gap ratio in the O band, $2\Delta_{01}/k_B T_c$, takes similar values as in the single-band model: for the case shown in Fig. 4, $2\Delta_{01}/k_B T_c=3.92$, somewhat greater than the BCS value. The ratio of the two zero-temperature gaps in Fig. 4 is $\Delta_{01}/\Delta_{02} \sim 3.4$. This ratio is very sensitive to V_{12} and the interactions in the bands, and, in fact, $V_{12}=0.2$ was chosen so as to give good qualitative agreement with the observation of two gaps reported in tunneling measurements recently.[6] When repulsive interactions are included in the Cu band, the Cu band gap is significantly suppressed, as will be shown below.

The exponential dependence at low temperatures in the specific heat will be governed by the smaller gap and therefore will occur on a much reduced temperature scale

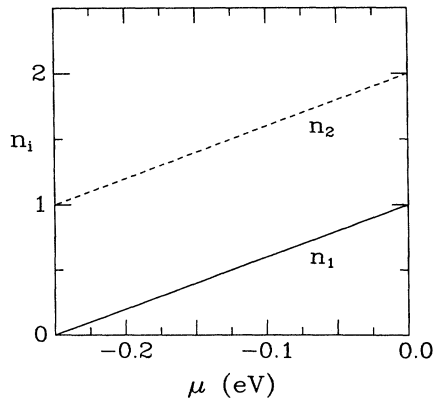

FIG. 3. n_1 and n_2 vs μ at $T=0$ for the case used in this paper: $D_1=D_2=0.5$ eV with a shift $\varepsilon_0=D_1/2$ as described in the text.

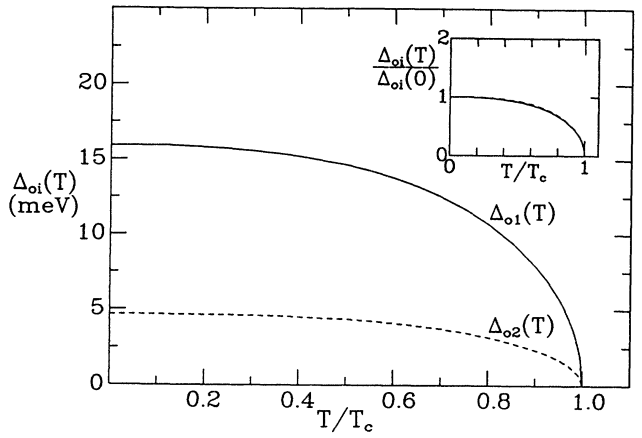

FIG. 4. The two gaps, $\Delta_{01}(T)$ and $\Delta_{02}(T)$ vs T/T_c for the case described in Fig. 2, with $n_1=0.12$. The parameters give a zero temperature ratio $\Delta_{01}(0)/\Delta_{02}(0)=3.4$. The inset shows the normalized gaps in both cases. The temperature dependence is identical and very similar to the usual BCS behavior.

in our model. In Fig. 5 we plot the specific heat versus temperature in both the superconducting and normal states. Also plotted are the respective single-band results obtained by setting $V_{12}=0$ and removing the Cu band. The single-band results display an exponentially suppressed low temperature specific heat in the superconducting state over a temperature range which is some sizable fraction of $T_c(\sim\frac{1}{3})$. The two-band results show a very restricted range over which the specific heat is exponential, followed by an approximately linear regime where the temperature is high enough that quasiparticles

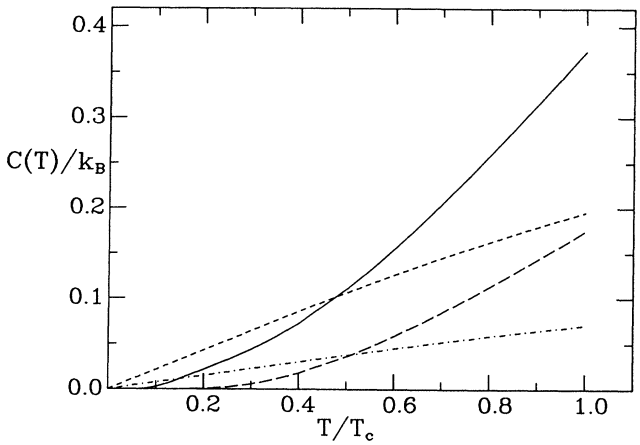

FIG. 5. Electronic specific heat vs reduced temperature for (1) the two-band model parameters of Fig. 2 in the superconducting (solid line) and normal (short-dashed line) states and for (2) the single-band model (same parameters, but $V_{12}=0$) in the superconducting (long-dashed line) and normal (dashed-dotted line) states. Note that the two-band case gives rise to exponential behavior in the superconducting state only at very low temperature, on the scale of the smaller gap.

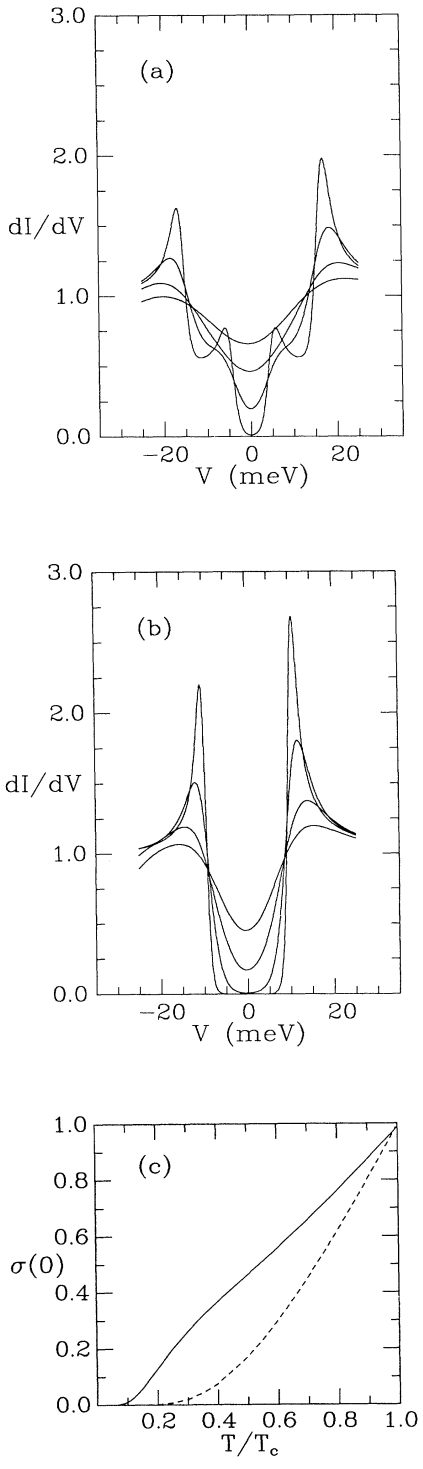

FIG. 6. (a) Plot of dI/dV vs V for the two-band model (parameters in Fig. 2 caption) at $T/T_c=0.1$, 0.25, 0.50, and 0.70. Note the two-gap structure resembling the tunneling data of Ref. 6. (b) Same plot for the single-band case, for the same reduced temperatures, shown for comparison. (c) Plot of the zero bias conductance, $\sigma(0)\equiv dI/dV(V=0)$ vs reduced temperature for the two cases shown in (a) (solid line) and (b) (dashed line). Note the much more rapid "filling in of the gap" with temperature in the two-band case as compared to the single-band model.

are easily excited across the smaller gap.

In this two-band model the size of the normalized specific heat jump $\Delta C(T_c)\equiv[C_s(T_c)-C_N(T_c)]/C_N(T_c)$ is considerably reduced from that obtained within weak coupling BCS theory [$\Delta C(T_c)=1.43$]. This is a consequence of the fact that if the Cu-band gap is very small then the Cu band appears to be normal for all practical purposes at T_c, so that $C_{S2}(T_c)\sim C_{N2}(T_c)$. Since $C_S=C_{S1}+C_{S2}$, and similarly for the normal state, and in this case the bandwidths are equal ($D_1=D_2$), then $\Delta C(T_c)\sim\frac{1}{2}(1.43)$ in the limit $\Delta_{02}\ll\Delta_{01}$ The normalized jump for the two-band case shown in Fig. 5 is $\Delta C(T_c)=0.90$.

The presence of a smaller gap in the two-band model will also affect the shape and temperature dependence of the current-voltage characteristic obtained through tunneling measurements. In Fig. 6(a) we display dI/dV (normalized to the normal state value) vs V for the two-band case, for various temperatures, and the single band result ($V_{12}=0$) in Fig. 6(b). The asymmetry found in the single-band case[1] remains in the peaks due to the larger gap; the smaller gap does not display an asymmetry because of the fact that we have taken the hopping interaction $K_2=0$ in the Cu band. Figure 6(a) bears a good qualitative resemblance to the data presented in Ref. 6, although the asymmetry observed there is of opposite sign to that predicted in our model (in our case, the larger peak occurs when holes are injected into the sample). In the two-band case structure due to the smaller gap occurs and leads to a significantly faster filling in of the "gap" with temperature compared to the single-band case, as seen in Fig. 6(c), where we plot the zero bias conductance, $\sigma(0)\equiv dI/dV(V=0)$ vs temperature for both the two-band and single-band cases.

B. Dependence on parameters

In this subsection we discuss how the results shown above are modified for other parameter values. It is generally found that the interactions in the second (Cu) band have little effect on T_c over most of the parameter range, while coupling V_{12} can strongly enhance T_c. (In fact, an extreme case of this behavior was discussed by Suhl *et al.*, where superconductivity was driven purely by V_{12}, with no attractive interactions in either band.)

On the other hand, the interactions in the Cu band have a strong effect on the size of the gap in that band. As a typical example, to contrast with the results in the previous subsection, we choose the interactions in the O and Cu bands equal: $K_1=K_2=1.63$ eV, $U_1=U_2=5$ eV, and $V_{12}=0.5$ eV. The magnitude of K was again chosen to give a maximum T_c somewhat above 90 K.

Figure 7 shows T_c versus n_1 for this case. Again it follows the qualitative behavior seen in the single-band model, with some enhancement occurring due to V_{12}. To illustrate the dependence of T_c with respect to the interactions in the Cu band we show in Fig. 8(a) the dependence on the on-site repulsion U_2 for two values of K_2. It is noteworthy that K_2 slightly enhances T_c despite the fact that the Cu band is less than half-full (with elec-

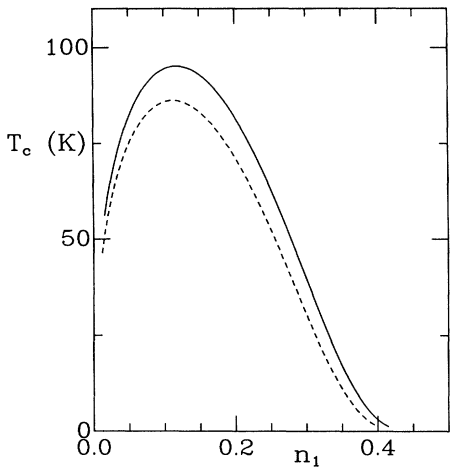

FIG. 7. T_c vs n_1 for the two-band model (solid line) and single-band model (dashed line) for the case when Cu and O interaction parameters are equal. We have used $D_1=D_2=0.5$ eV, $K_1=K_2=1.63$ eV, and $U_1=U_2=5.0$ eV, with $V_{12}=0.5$ eV in the two-band case and $V_{12}=0$ in the single-band case. The conclusion is the same as in Fig. 2. The extra band does not qualitatively change the single-band result.

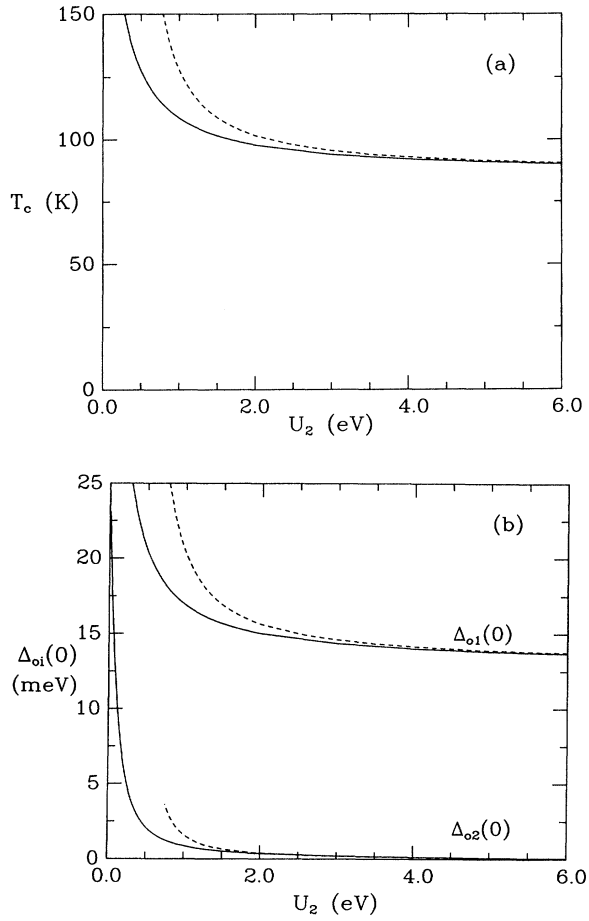

FIG. 8. (a) T_c vs U_2 for fixed parameters: $D_1=D_2=0.5$ eV, $K_1=1.63$ eV, and $U_1=5.0$ eV. The curves represent solutions with $K_2=0$ (solid line) and $K_2=0.8$ eV (dashed line). Note that for sizable $U_2 \gtrsim 2$ eV T_c is insensitive to both U_2 and K_2. (b) The gaps Δ_{01} and Δ_{02} for both $K_2=0$ (solid line) and $K_2=0.8$ eV (dashed line) as a function of U_2. Both gaps are insensitive to the choice of K_2 for $U_2 \gtrsim 2$ eV. Note that as U_2 increases Δ_{01} becomes constant whereas Δ_{02} is driven monotonically to zero.

trons). In Fig. 8(b) we plot the gaps in each band as a function of U_2. In a small range close to $U_2=0$ the interaction U_2 can suppress T_c and Δ_{01} by about a factor of 2; on the other hand this is easily compensated for by a small change in K_1 or U_1. For larger values of U_2, T_c and Δ_{01} are insensitive to changes in the Cu band interactions. In contrast U_2 drives Δ_{02} rapidly to zero, as seen in Fig. 8(b). It is possible that other interactions not included in the model or inclusion of correlation effects beyond BCS theory in the Cu band could alter this result.

In Fig. 9 we show the gaps versus temperature for the case shown in Fig. 7 (equal interactions in O and Cu bands) and chemical potential such that T_c is maximum ($n_1=0.12$, $n_2=1.12$). The zero-temperature gap in the Cu band is very small here: $\Delta_{01}/\Delta_{02}=95$, due to the effect of U_2. The temperature dependence of the Cu band gap is also significantly altered, as shown in the inset in Fig. 9. In the presence of a sizable U_2 it is found that the gap in the Cu band remains small even for large V_{12} (for example, $V_{12}=2$ decreases the ratio to $\Delta_{01}/\Delta_{02}=18$ only).

Next we show the behavior of specific heat and tunneling characteristics in the presence of the very small gap. As seen in Fig. 10, the specific heat appears to be linear now at low temperatures over a significant temperature range, and the specific heat jump is further reduced, to $\Delta C(T_c)=0.77$. The tunneling characteristics in Fig. 11 display the existence of the second gap only for very low temperatures ($T \leq 0.05 T_c$); for higher temperatures the small gap has been filled in and the larger gap structure appears to be superposed on a normal state background. Such a "zero bias anomaly" is reported in various tunneling studies of high-T_c superconductors.[4] However, we believe the case discussed in the previous subsection with a larger second gap is likely to be more appropriate to describe the situation in the high-T_c oxides.

To conclude, we emphasize that in these calculations the bandwidths of the Cu and O bands have been kept fixed when varying the hole concentration, which is why T_c is found to be nonzero over a substantially larger hole concentration range than seen experimentally. As discussed in Ref. 1, the effective bandwidth in the O band should increase linearly with hole concentration due to the effect of K_1 on the effective single particle hopping, and one may expect similarly an increase in the effective bandwidth of the Cu band as one moves away from the strongly correlated half-filled band case. In the single-band case it was found that inclusion of this effect reduces the range of hole concentration where T_c is nonzero by about a factor of 2, leaving the shape of the T_c versus N curve qualitatively unchanged. An identical behavior is found in the two-band model discussed here due to bandwidth renormalization of the O band (bandwidth renormalization of the Cu band has a minor effect).

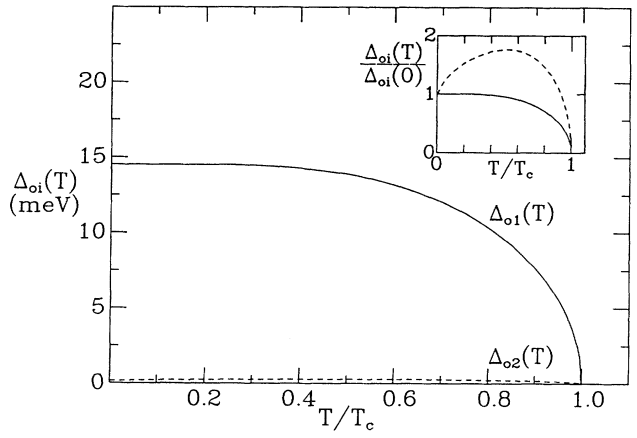

FIG. 9. Plot of two gaps vs reduced temperature for the two-band model with parameters given in the caption of Fig. 7. The ratio $\Delta_{01}(0)/\Delta_{02}(0)=95$ is much higher than in Fig. 4 due to the repulsive interactions present in the Cu band. The inset shows the peculiar temperature dependence of the small Cu band gap (dashed line).

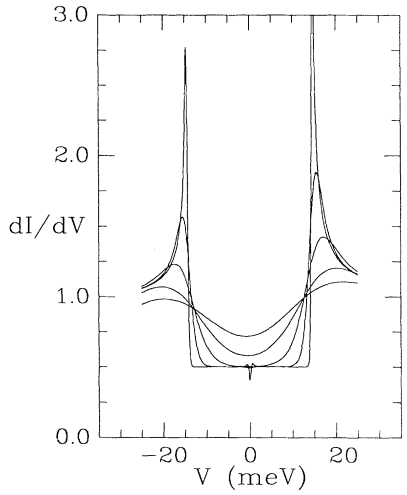

FIG. 11. Plot of dI/dV vs V for the parameters of Fig. 7 for $T/T_c=0.02$, 0.10, 0.25, 0.50, and 0.70. Note that the small gap is immediately filled in with increasing temperature, giving rise to a "background conductivity."

IV. HALL COEFFICIENT

A. Normal state

Expressions for the low-field Hall coefficient in a multiband model are given, for example, in Allen *et al.*[10] Within our two-band model for a magnetic field applied perpendicular to the *ab* plane, they reduce to

$$R_{ab}^{H}=\frac{\sigma_{abc}}{\sigma_{ab}^{2}}\ , \tag{14a}$$

$$\sigma_{abc}=-e^{3}\tau^{2}\sum_{i}\int_{-\infty}^{\infty}d\varepsilon\ g_{xxy}^{i}(\varepsilon)\left[\frac{-\partial f}{\partial\varepsilon}\right], \tag{14b}$$

$$\sigma_{ab}=e^{2}\tau\sum_{i}\int_{-\infty}^{\infty}d\varepsilon\ g_{xx}^{i}\left[\frac{-\partial f}{\partial\varepsilon}\right], \tag{14c}$$

where

$$g_{xx}^{i}(\varepsilon)\equiv\frac{1}{N}\sum_{k}\left[\frac{D_i}{4}\sin k_x\right]^{2}\delta(\varepsilon-\varepsilon_{ki}) \tag{15a}$$

and

$$g_{xxy}^{i}(\varepsilon)\equiv\frac{1}{N}\sum_{k}\left[\frac{D_i}{4}\sin k_x\right]^{2}\left[\frac{D_i}{4}\cos k_x\right]\delta(\varepsilon-\varepsilon_{ki}) \tag{15b}$$

are weighted densities of states. We have assumed the scattering time τ is constant in both bands, and as before, "i" is the band index. Using parabolic expansions of the band energies near the bottom and top of the bands and then interpolating gives rise to the following effective weighted densities of states within the "constant density of states model:"

$$g_{xx}^{i}(\varepsilon)=\frac{D_i}{8}\left[1-\left[\frac{\varepsilon}{D_i/2}\right]^{2}\right], \tag{16a}$$

$$g_{xyz}^{i}(\varepsilon)=\frac{-1}{2}\frac{\varepsilon}{D_i/2}\left[\frac{D_i}{4}\right]^{2}\left[1-\left[\frac{\varepsilon}{D_i/2}\right]^{2}\right], \tag{16b}$$

where as before, within each band energy is measured with respect to the middle of that band. At $T=0$ we use

$$n_i=2+\frac{\mu+\varepsilon_0^{i}}{D_i/2} \tag{17}$$

for the number of occupied holes in each band so that the Hall coefficient becomes

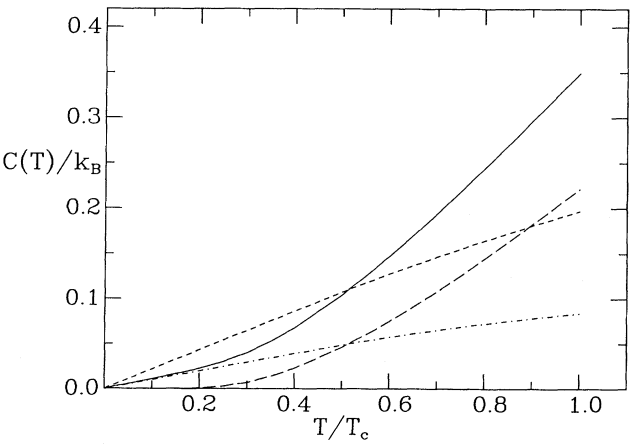

FIG. 10. Plot of specific heat vs reduced temperature for (1) the two-band model (with parameters in the caption of Fig. 7) in the superconducting (solid line and normal (short-dashed line) states and (2) the single-band model (with same parameters but $V_{12}=0$) in the superconducting (long-dashed) and normal states. Note that the temperature dependence of the two-band specific heat in the superconducting state is almost linear down to $T=0$.

$$R_{ab}^{H}=\frac{2}{e}\frac{[(1-n_1)n_1(2-n_1)-(D_2^2/D_1^2)(n_2-1)n_2(2-n_2)]}{[n_1(2-n_1)+(D_2/D_1)n_2(2-n_2)]^2} . \tag{18}$$

Since $D_2/D_1=\mu_2/\mu_1$, where μ_i is the mobility for each band, expression (18) reduces to the usual two-band result in the parabolic limit, i.e., $n_1\to 0$ and $n_2\to 2$.

Using equal densities of states for both bands, then from Eq. (17) or Fig. 2 it is apparent that for a given chemical potential, $n_2=1+n_1$, so that for small n_1 R_{ab}^{H} is positive whereas beyond $n_1=0.5R_{ab}^{H}$ becomes negative. This change of sign coincides roughly with the depression to zero of T_c seen in Fig. 2, in agreement with experiment.[11] In Fig. 12 we plot R_{ab}^{H} as a function of the total occupancy. At zero temperature there is a decrease in the Hall coefficient near $n_{\rm tot}=1$, in disagreement with observations. This occurs because we have not taken into account the opening of a Mott-Hubbard gap. Otherwise, the single-band model for conducting holes would apply yielding a diverging positive Hall coefficient, as seen in experiment.[4,11]

B. Superconducting state

The Hall coefficient near T_c exhibits peculiar behavior in the oxides, as recently pointed out by several authors.[8,9] Here we use a simple argument to derive the qualitative behavior of the Hall coefficient in our model in the superconducting state, in the spirit of the "local model" of Bardeen and Stephen.[12] A related analysis has been given by Ho[13] in a model with electrons and holes.

Within the Bardeen-Stephen model the contribution to the Hall voltage in the mixed state arises from the "normal electrons" inside the vortex cores. The Hall angle θ (the angle between the electric field direction and the direction of the transport current) is the same as in the normal state for a one-component system in this model. Now the ratio of normal electrons (inside the core) to total number of electrons can be taken to be

$$\frac{n_n}{n_T}=\frac{B}{H_{c2}} , \tag{19}$$

with B the magnetic induction and H_{c2} the upper critical field. This relation follows from the facts that the density of vortex lines is given by B/ϕ_0, with ϕ_0 the flux quantum (since each vortex line carries one quantum of flux) and that H_{c2} is the field at which different vortex cores start to overlap. As a function of applied magnetic field H, $B=0$ for $H\le H_{c1}$ and $B\sim H$ for $H\gg H_{c1}$. For our purposes, since $H_{c1}\ll H_{c2}$ in these materials we will neglect the distinction between B and H. The upper critical field is given by

$$H_{c2}=\frac{\phi_0}{2\pi\xi^2} , \tag{20}$$

with ξ the (Ginzburg-Landau) coherence length. Since the coherence length is related to the superconducting gap Δ by

$$\xi\sim\frac{\hbar v_F}{\Delta} \tag{21}$$

($v_F=$ Fermi velocity), we expect from Eq. (19) that the number of normal electrons is inversely proportional to the square of the gap parameter.

Within our two-band model electrons and holes have widely different gaps. Quite generally, as discussed in the previous section, we expect holes to have a substantially larger gap parameter than the electrons. Thus, for small magnetic fields, the electrons will become "normal" more readily than the holes and the Hall coefficient will tend to be negative, switching to positive values (as in the normal state) at larger fields as the holes also become normal. Such is the behavior seen experimentally.

To make these remarks more quantitative we use a simplified expression for the (low field) Hall angle, assuming equal mobility in both bands:

$$\tan\theta=CH\frac{n_1^{\rm eff}(T,H)-n_2^{\rm eff}(T,H)}{n_1^{\rm eff}(T,H)+n_w^{\rm eff}(T,H)} , \tag{22}$$

with C a constant (independent of T and H),

$$n_i^{\rm eff}(T,H)=\frac{H}{H_{c2}^{i}(T)}n_i^{\rm eff} \quad H\le H_{c2}(i)$$
$$=n_i^{\rm eff} \quad H>H_{c2}(i) , \tag{23}$$

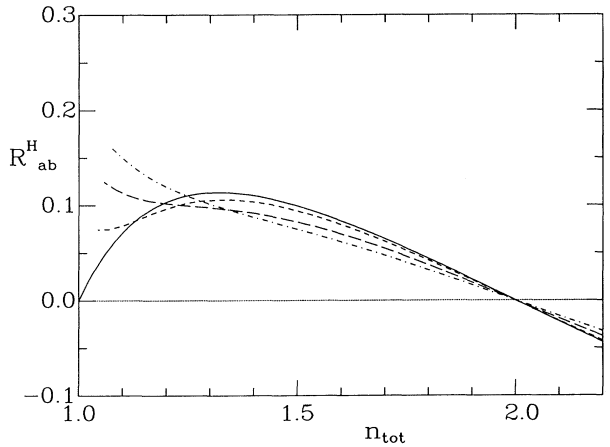

FIG. 12. Normal state Hall coefficient vs total occupation $n_{\rm tot}$ for $T=0$ (solid line), $T=100$ K (short-dashed), $T=200$ K (long-dashed), and $T=300$ K (dot-dashed). At $T=0$ the Hall coefficient goes to zero at $n_{\rm tot}=1.0$ ($n_1=0$, $n_2=1$) due to the presence of the Cu band. A gap in the Cu band would give rise to diverging Hall coefficient (single-band result). The Hall coefficient is positive at low concentration and changes sign at $n_{\rm tot}=2$ ($n_1=0.5$), where T_c goes to zero (see Figs. 2 or 7), in agreement with experiment. We have used $D_1=D_2=0.5$ eV.

and the values of $n_i^{\rm eff}$ chosen to reproduce the behavior of the zero-temperature Hall coefficient in the normal state given by Eq. (18), i.e.,

$$\frac{n_1^{\rm eff}}{n_2^{\rm eff}}=\frac{(1-n_1)n_1(2-n_1)}{(n_2-1)n_2(2-n_2)} . \tag{24}$$

The upper critical fields are chosen to satisfy

$$\frac{H_{c2}^1(T)}{H_{c2}^2(T)}=\left[\frac{\Delta_{01}(T)}{\Delta_{02}(T)}\right]^2 , \tag{25}$$

following Eqs. (20) and (21), with Δ_{0i} given in Eq. (13). As an illustrative example we choose

$$\frac{H_{c2}^1(0)}{H_{c2}^2(0)}=10 \tag{26a}$$

and

$$\frac{n_1^{\rm eff}}{n_2^{\rm eff}}=2 , \tag{26b}$$

which are close to our "simple example" in Sec. III. There, at the peak in the T_c versus n_1 curve, $T_c=94.1$ K, $n_c=0.12$, and $n_d=1.12$ so that $n_1^{\rm eff}=0.20$, $n_2^{\rm eff}=0.12$. Furthermore, $[\Delta_{01}(0)/\Delta_{02}(0)]^2=11.6$. The temperature dependence of $\Delta_{01}(T)$ is taken from Fig. 4 and the ratio $\Delta_{01}(T)/\Delta_{02}(T)$ is assumed to be temperature independent which is an excellent approximation in this parameter range (see inset in Fig. 4). Finally, to set the scale of magnetic fields we take

$$H_{c2}^1(0)=100 \text{ T} , \tag{27}$$

which is in the range of various estimates for H_{c2},[4] and corresponds to a coherence length $\xi=18$ Å.

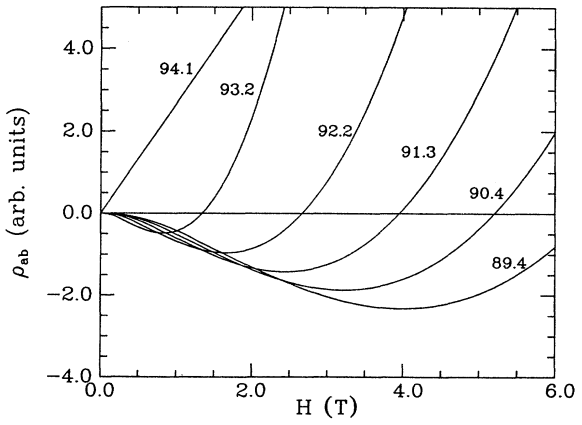

FIG. 13. Plot of Hall resistivity, ρ_{ab} vs magnetic field H, for various temperatures indicated. In the superconducting state the Hall resistivity is first negative and then changes sign, in good qualitative agreement with experiments (Refs. 8 and 9). The numbers next to the curves give the temperature in K. $T_c=94.1$ K.

Figure 13 shows the results for the Hall resistivity

$$\rho_{ab}=\tan\theta\rho_{aa}$$

versus applied magnetic field H for a set of temperatures close to T_c for this case. We assume the longitudinal resistivity ρ_{aa} to be proportional to $H/H_{c2}^1(T)$.[12] The vertical scale is left arbitrary due to the uncertainties involved in our calculation. Our results do not reproduce the regime of zero Hall resistivity observed at low fields,[8] which is presumably related to pinning effects. Nevertheless, the overall behavior does resemble the experimental observations,[8,9] including the scale of magnetic fields and temperatures involved. A change in either ratio Eq. (26a) or Eq. (26b) results in a change in the scale of H in Fig. 13.

The scale of the curves displayed in Fig. 13 is set by the larger upper critical field $H_{c2}^1(T)$. Within our approximation the magnetic field where the Hall constant changes sign is given by

$$H_0(T)=\frac{n_2^{\rm eff}}{n_1^{\rm eff}}H_{c2}^1(T) , \tag{28a}$$

and the minimum in the Hall resistivity is attained at

$$H_{\rm min}^{(T)}=\left[\frac{\sqrt{5}-1}{2}\right]\frac{n_2^{\rm eff}}{2n_1^{\rm eff}}H_{c2}^1(T) \tag{28b}$$

so that we would predict $H_{\rm min}=0.62H_0$. This is only in rough agreement with experimental observations. We note, however, that there is significant scatter in the different results reported[8,9] and, in fact, $H_{\rm min}$ is sometimes above and sometimes below this value. There could also be systematic corrections to Eq. (28) from finite-field corrections to the low-field Hall coefficient expression used. Finally, we note that both H_0 and $H_{\rm min}$ are proportional to $H_{c2}^1(T)$ so that they should be approximately linear in (T_c-T), except for the deviations due to the curvature of $H_{c2}(T)$ observed experimentally.[4] This is also approximately consistent with the results reported for the Hall resistivity.

V. DISCUSSION

We have used a two-band model to describe certain aspects of superconductivity in the high-T_c oxides. The principal motivation for this work was to incorporate the relevant Copper degrees of freedom into the single-band oxygen-hole description of Ref. 1. Since these degrees of freedom give rise to the antiferromagnetism of the insulating phase the question naturally arises as to what role they play in the superconducting regime: they cannot be totally decoupled, as one would not expect Cu local moments to survive in the superconducting state.

Experiments,[4] as well as numerical simulations of model Hamiltonians[14] indicate that antiferromagnetism disappears very rapidly as the systems are doped. Hence we have assumed here that away from the insulating state the Cu band is described by a Fermi liquid, which is not inconsistent with either experiments or simulations. The question then arises as to how the carriers in the Cu band

take part in the superconducting state, under the assumption that there is no pairing interaction in that band. We have used the interaction term introduced by Suhl *et al.* as the simplest way to deal with this situation.

We wish to emphasize here that our treatment has not taken into account the possible effects of impurity scattering. For example, as reviewed by Gladstone *et al.*,[15] in the "dirty limit" (mean free path less than coherence length) multiband effects are expected to be unimportant in superconductors. In good quality high-T_c samples, because of the very short coherence length, one expects to be in the opposite "clean limit," where multiband effects can be important. Nevertheless, impurity scattering could somewhat alter the behavior of thermodynamic properties discussed in Sec. III, particularly since we expect impurity scattering to be especially relevant in the model discussed here due to the energy dependence of the gap.[16,1] Thus, in comparing experimental results with the theory discussed here it is important that high purity samples be used. We plan to discuss the effect of impurity scattering in this theory in future work.

The first conclusion of the present study is that, in fact, the Cu degrees of freedom can be incorporated into the problem in a way that leaves the major features of the single-band model of Ref. 1 unchanged. The energy dependence of the gap in the O band, the gap to T_c ratio, and the dependence of T_c on O hole concentration as well as on interaction parameters in the O band (and hence on pressure, for example), are left essentially unchanged in the present model. The magnitude of T_c is not strongly affected by the interband interaction and the interactions in the Cu band. Furthermore, although we have only presented results for the simplest situations it is clear that the features found in Ref. 1 on incorporating an anisotropic band structure, nearest-neighbor Coulomb repulsion, and band-renormalization effects carry over directly to the two-band model.

The second conclusion is that the presence of the second band gives rise to a second energy gap, smaller than the first, associated with the Cu band, that is driven by the attractive interaction in the O band. The size of this gap is very sensitive to both the interactions in the Cu band and the interband coupling and is not simply related to the magnitude of T_c. In fact, it can be much smaller than T_c, leading to a modification of various properties of the system in the superconducting state due to the fact that low-lying quasiparticle excitations in that band exist. Here we have examined the behavior of specific heat and tunneling characteristics and shown that the second gap gives rise to observable effects which are in qualitative agreement with some observations. There are a variety of other observables that will be modified by the presence of a second gap, which will be discussed elsewhere.

There have been, in fact, discussions in the literature about the possible existence of two gaps in the oxide superconductors.[4,6,17] However, these have been associated with structural features of these materials, either with chains and planes in the $YBa_2Cu_3O_7$ structure[17] or with different gaps for in-plane and perpendicular-to-plane directions.[6] It should be emphasized that in our model the two gaps are intrinsic, independent of structural features, and are expected to be isotropic,[1] i.e., constant over the Fermi surface. High resolution photoemission experiments should eventually be able to decide between the different pictures: our model specifically predicts no significant k- dependence to the gap structures observed.

Finally we come to what may well turn out to be the prime evidence in the high-T_c puzzle, the behavior of the Hall coefficient near the critical temperature. The change in sign in the Hall coefficient from negative to positive as the magnetic field is increased[8,9,18] or the temperature is increased[19] near T_c has been observed in a variety of samples and interpreted using widely different assumptions: vortex motion in direction opposite to the transport current,[9] rapid variation of quasiparticle normal properties in the region around superconductivity onset,[8,13] and effects associated with grain boundaries,[19] or with different orientation of grains in polycrystalline samples.[8] Our model suggests a simpler and more fundamental explanation: if pairing of hole carriers drives the superconductivity and the existing electron carriers are merely carried along, as described by the present model, it will naturally be easier to break up the electron carrier pairs through a magnetic field or temperature, leading to a negative Hall coefficient that reverts to its normal-state positive value as the hole-carrier pairs also break up at higher temperatures or fields. The simple analysis of Sec. IV yielded qualitative agreement with observations, and a more detailed analysis should allow for quantitative comparison. In particular, a prediction of our model is that both H_0 and $H_{\min}$ [Eq. (28)] should decrease faster than the upper critical field as the hole concentration is increased, due to the change in $n_2^{\text{eff}}/n_1^{\text{eff}}$ [Eq. (24)]. It is not clear whether the alternative explanations offered[8,9,19] would predict similar behavior, and the existing experimental results do not address this issue.

It is pointed out in Ref. 8 and emphasized by Hagen *et al.*[9] that this sign reversal of the Hall coefficient is also observed in low-temperature elemental superconductors such as Nb and V. For this reason Hagen *et al.* sought to explain the effect in a way that would apply both to the high-T_c materials as well as to "conventional" superconductors. We note that the ideas put forth in Ref. 20 similarly imply a unified explanation of the phenomenon along the lines discussed in this paper.

ACKNOWLEDGMENTS

This work was supported by National Science Foundation (NSF) Grant No. DMR-8918306.

*Present address: Theoretical Physics Branch, AECL Research, Chalk River Laboratories, Chalk River, Ontario K0J 1J0, Canada.

[1]J. E. Hirsch and F. Marsiglio, Phys. Rev. B **39**, 11 515 (1989); F. Marsiglio and J. E. Hirsch, *ibid.* **41**, 6435 (1990).

[2]J. E. Hirsch and S. Tang, Phys. Rev. B **40**, 2179 (1989); J. E. Hirsch and F. Marsiglio, *ibid.* **41**, 2049 (1990).

[3]Y. Guo, J. M. Langlois, and W. A. Goddard III, Science **239**, 896 (1988); see, also, J. E. Hirsch and S. Tang, Solid State Commun. **69**, 987 (1989).

[4]See various experimental papers, in Proceedings of the International Conference on Materials and Mechanisms of Superconductivity, High Temperature Superconductors II, Stanford, 1989, edited by R. N. Shelton, W. A. Harrison, and N. E. Phillips [Physica C **162-164** (1989)]; and Proceedings of the International Conference on High Temperature Superconductors and Materials and Mechanisms of Superconductivity, Interlaken, Switzerland, 1988, edited by J. Müller and J. L. Olsen [Physica C **153-155** (1988)].

[5]H. Suhl, B. T. Matthias, and L. R. Walker, Phys. Rev. Lett. **3**, 552 (1959).

[6]M. Gurvitch *et al.*, Phys Rev. Lett. **63**, 1008 (1989).

[7]J. R. Kirtley, Int. J. Mod. Phys. **4**, 201 (1990).

[8]M. Galffy and E. Zirngiebl, Solid State Commun. **68**, 929 (1988).

[9]S. J. Hagen *et al.*, Phys. Rev. B **41**, 11 630 (1990).

[10]P. B. Allen, W. E. Pickett, and H. Krakauer, Phys. Rev. B **37**, 7482 (1988).

[11]H. Takagi *et al.*, Phys. Rev. B **40**, 2254 (1989).

[12]J. Bardeen and M. J. Stephen, Phys. Rev. **140**, A1197 (1965).

[13]L. C. Ho, Can. J. Phys. **48**, 1939 (1970).

[14]J. E. Hirsch and S. Tang, Phys. Rev. Lett. **62**, 591 (1989); A. Moreo *et al.*, Phys. Rev. B **41**, 2313 (1990); R. T. Scalettar *et al.* (unpublished).

[15]G. Gladstone, M. A. Jensen, and J. R. Schrieffer, in *Superconductivity,* edited by R. D. Parks (Marcel Dekker, New York, 1969), Vol. II, p. 665.

[16]L. Coffey and D. L. Cox, Phys. Rev. B **37**, 3389 (1987).

[17]W. W. Warren *et al.*, Phys. Rev. Lett. **59**, 1860 (1987).

[18]Y. Iye, S. Nakamura, and T. Tamegai, Physica C **159**, 616 (1989).

[19]Z. Yong *et al.*, Solid State Commun. **65**, 885 (1987); T. Hiraoka, Jpn. J. Appl. Phys. **28**, 21 135 (1989).

[20]J. E. Hirsch, Physica C **158**, 326 (1989); Phys. Lett. A **138**, 83 (1989).